Generalized Sturmian Functions applied to double continuum problems

2015 J. Phys.: Conf. Ser. 601 012004

(http://iopscience.iop.org/1742-6596/601/1/012004)

Generalized Sturmian Functions applied to double continuum problems

M. J. Ambrosio[1,5], F. D. Colavecchia[2,5], D. M. Mitnik[1,5], G. Gasaneo[3,5] and L. U. Ancarani[4]

[1] Instituto de Astronomía y Física del Espacio, Argentina.
[2] División Física Atómica, Molecular y Óptica, Centro Atómico Bariloche, 8400 S. C. de Bariloche, Río Negro, Argentina.
[3] Departamento de Física, Universidad Nacional del Sur, 8000 Bahía Blanca, Buenos Aires, Argentina.
[4]Théorie, Modélisation, Simulation, SRSMC, UMR CNRS 7565, Université de Lorraine, 57078 Metz, France
[5] Consejo Nacional de Investigaciones Científicas y Técnicas, CONICET, Argentina.

E-mail: mja1984@gmail.com

Abstract. The Generalized Sturmian Functions method aims to deal with atomic physics problems. It has seen application to two and three–body problems, and its flexibility enables one to work with bound systems as well as with particles in the continuum. In the present contribution we analyze how the method expands the atomic double continuum in collision problems, using the double ionization of Helium by fast electrons as a showcase. We first test the robustness of the method in a particularly challenging situation, the zero energy case. We then present fully differential cross sections for a scattering problem which after 15 years of continued efforts has not been satisfactorily solved: the double ionization of Helium by electron impact in the fast projectile regime, as measured by the Orsay group.

1. Introduction

The Generalized Sturmian Functions (GSF) methodology was introduced seven years ago [1], and has seen a series of successful applications in atomic physics problems (see [2] and references therein). Whether in the case of bound systems or particles in the continuum, the method has provided accurate solutions at a computationally inexpensive cost (see, e.g., Ref. [3]). GSF form basis sets which have two main characteristics underlying their efficiency. First, the basis functions can be constructed in such a way to contain the exact or approximate asymptotic conditions for a given problem. Second, the oscillations of the basis functions can be localized in any spatial region of interest, leaving the expansion to deal essentially with the domain where it is most needed.

For the case of bound systems, it is easy to understand how the basis functions provide excellent convergence properties, concentrating the expansion capabilities in the (inner) region of interest [4, 5, 6, 7] and having all basis elements decay exponentially at the same rate, as close as possible to the expected behavior of the physical wave function.

Less clearly established is how the basis manages to solve three–body double continuum problems, although the efficiency has been illustrated through application to the study of

single electron impact ionization of hydrogen [3, 8]. This contribution aims to analyze how the hyperspherical asymptotic behavior for the double continuum wave fronts can be well approximated by the GSF method, by using an angularly coupled combination of basis functions in the radial coordinates of the two emitted particles.

The proposed analysis is done here for the double ionization of Helium in the fast projectile regime. This process is formally a four–body problem, but the collision dynamics can be reduced to a three–body problem when treating the projectile in a perturbative fashion [9]. For the purpose of the present investigation, in the first part we restrict ourselves to a Temkin–Poet (TP) model of the physical process. While keeping the main challenges of a three–body problem, it allows to perform studies on a single partial wave. Then, going beyond the TP case, the full three–body problem is studied and Fivefold Differential Cross Sections (FDCS) are briefly presented. We also provide some convergence details related to the relevance of angular momentum partial waves.

Atomic units ($\hbar = e = m_e = 1$) are assumed throughout, unless stated otherwise.

2. Double ionization of Helium by fast electrons: GSF expansion

The double ionization of Helium formalism used by our group was introduced in [9]. The system is comprised of the nucleus ($Z = 2$), the target electrons and the projectile. With the same notation as in Ref. [9, 10, 11], r_2 and r_3 denote the distances between the nucleus and the target electrons, and r_{23} the interelectronic distance. Vector $\mathbf{q}$ stands for the momentum transferred from the projectile to the originally bound system; in this work we shall take $q = 0.24$ a.u. which corresponds to one of two configurations explored by the Orsay group in Refs. [12, 13, 14]. The Helium target is left with total energy E_a after the collision. The formulation treats the projectile–He interactions in a perturbative fashion [9]; considered up to its first order, it yields the following equation for the ejected electrons' scattering wave function:

$$\left[h_{He} - E_a\right] \Phi^{+}_{sc}\left(\mathbf{q}, \mathbf{r}_2, \mathbf{r}_3\right) = -\frac{4\pi}{q^2} \frac{1}{(2\pi)^3} \left(-Z + e^{i\mathbf{q}\cdot\mathbf{r}_2} + e^{i\mathbf{q}\cdot\mathbf{r}_3}\right) \Phi_i\left(\mathbf{r}_2, \mathbf{r}_3\right), \tag{1}$$

where the three–body Hamiltonian h_{He} is given by

$$h_{He} = \left(-\frac{1}{2}\nabla_2^2 - \frac{1}{2}\nabla_3^2 - \frac{Z}{r_2} - \frac{Z}{r_3} + \frac{1}{r_{23}}\right). \tag{2}$$

The Hamiltonian appearing in Eq. (1) is separable in the total angular momentum subspaces, implying that the well known bipolar harmonics $\mathcal{Y}^{LM}_{l_2 l_3}\left(\widehat{\mathbf{r}}_2, \widehat{\mathbf{r}}_3\right)$ are eigenfunctions of this operator. Consequently, we construct the three–body GSF basis $\Theta_\nu\left(\mathbf{r}_2, \mathbf{r}_3\right)$ as the non–correlated product (i.e., with no explicit r_{23} dependence)

$$\Theta_\nu\left(\mathbf{r}_2, \mathbf{r}_3\right) = \mathcal{Y}^{LM}_{l_2 l_3}\left(\widehat{\mathbf{r}}_2, \widehat{\mathbf{r}}_3\right) \frac{S_{n_2 l_2}\left(r_2\right)}{r_2} \frac{S_{n_3 l_3}\left(r_3\right)}{r_3}, \tag{3}$$

where index ν denotes the set of indices $\{L, M, l_2, l_3, n_2, n_3\}$. For three–body problems, the GSF method expands the continuum solution $\Phi^{+}_{sc}\left(\mathbf{r}_3, \mathbf{r}_3\right)$ in terms of this basis set:

$$\Phi^{+}_{sc}\left(\mathbf{q}, \mathbf{r}_2, \mathbf{r}_3\right) = \sum_{L,M} \sum_{l_a, l_b} \sum_{n_a, n_b} \phi_\nu \Theta_\nu\left(\mathbf{r}_2, \mathbf{r}_3\right), \tag{4}$$

with coefficients ϕ_ν. The two–body functions $S_{n_2 l_2}\left(r_2\right)$ and $S_{n_3 l_3}\left(r_3\right)$ in Eq. (3) are the so–called Generalized Sturmian Functions, and verify a homogeneous differential equation which resembles the reduced radial Schrödinger equation:

$$\left[\mathcal{T}_l + \mathcal{U}(r) - E_s\right] S_{nl}(r) = -\beta_{nl}\, \mathcal{V}(r)\, S_{nl}(r), \tag{5}$$

with $\mathcal{T}_l = -\frac{1}{2\mu}\frac{d^2}{dr^2} + \frac{l(l+1)}{2\mu r^2}$, μ the reduced mass (set to 1 throughout this paper) and l the angular momentum quantum number. The energy E_s is fixed externally, and in principle, is an arbitrary parameter. A good choice of E_s, however, plays a key role to describe the double continuum behavior, as will be discussed later. The potential $\mathcal{U}(r)$ is used to include in the basis set some physics of the problem in question: mainly to account for non–active electrons shielding the nuclear charge and for the asymptotic charge perceived at long ranges by the active electrons. The other potential involved in Eq. (5), $\mathcal{V}(r)$, is called *generating potential*, and its role is to concentrate the oscillations of the basis in any desired region, thus tailoring the set for any specific application.

Sturmians with negative E_s decay exponentially and are suitable for bound state studies. For positive E_s, the asymptotic behavior can be chosen as a linear combination of pure Coulombic waves $H_l^+(r)$ and $H_l^-(r)$. For continuum applications we choose $E_s > 0$ and $S_{nl}(r) \to H_l^+(r)$ beyond a given radius R. Past the point $r = R$, all basis elements become linearly dependent (LD) and exhibit the same asymptotic behavior.

As it has been shown in previous publications (see [2] and references therein), the GSF method is particularly efficient resource wise when dealing with three–body bound states, and also with the three–body continuum [3]. In this contribution it is our wish to further investigate why the methodology works well in building up the double continuum. The main point is the following. The GSF basis imposes outgoing (+) type asymptotic conditions on each coordinate r_2 and r_3, i.e., on a square contour in the (r_2, r_3) space. However, the double continuum asymptotic behavior comprises outgoing waves in the hyperradial coordinate $\rho = \sqrt{r_2^2 + r_3^2}$, i.e., on a circular contour. We will see below that, with an adequate choice of energy E_s for the basis set, the outgoing hyperspherical condition is very well approximated by the GSF implementation in spherical coordinates (r_2, r_3).

3. Double continuum asymptotic conditions

Ideally, for a double continuum wave function to be a proper solution of the three-body problem, the asymptotic conditions imposed by a resolution scheme should contain or approximate the hyperspherical behavior formally established by Peterkop [15] and Kadyrov [16, 17]. Thus, the pure hyperspherical double continuum should be imposed in order to perfectly expand the expected solution. This would imply a scattering function with an asymptotic wave vector given by $\boldsymbol{\kappa} = \kappa\widehat{\boldsymbol{\rho}}$, defining for the purpose $\widehat{\boldsymbol{\rho}} = \cos(\alpha)\ \widehat{\mathbf{e}}_2 + \sin(\alpha)\ \widehat{\mathbf{e}}_3$, $\kappa = \sqrt{2E_a}$, and where $\tan(\alpha) = r_3/r_2$. Unit vectors $\widehat{\mathbf{e}}_2$ and $\widehat{\mathbf{e}}_3$ point in the (r_2, r_3) space, respectively along axes r_2 and r_3.

In figure 1 we show the scattering wave function $\Phi_{sc}^+(\mathbf{q}, \mathbf{r}_2, \mathbf{r}_3)$, calculated within a RxR=60x60 a.u. box, but plotted beyond the range of the calculation, where the basis sets are no longer linearly independent (LI). Sector I is where the basis is LI in both coordinates. In sector II we are evaluating the function beyond the $r_2 = R$ limit, where the set $S_{n_2l_2}(r_2)$ has become LD and $S_{n_3l_3}(r_3)$ still has expanding capabilities (i.e., is LI); in sector III we have the symmetric situation. Sector IV shows $\Phi_{sc}^+(\mathbf{q}, \mathbf{r}_2, \mathbf{r}_3)$ plotted when the basis is, in both coordinates, outside of its LI range. It contains pure outgoing wave fronts. We stress here that the calculation is performed inside the box, and physical results (cross sections) are always extracted from within it.

Consider the transition from sector I to II. For $r_2 > R$, the GSF set $S_{n_2l_2}(r_2)$ behaves as an outgoing wave in coordinate r_2, becoming LD. But we are still inside the r_3 range where the elements $S_{n_3l_3}(r_3)$ are LI. Therefore, in the r_3 direction, the basis can expand the behavior of the expected hyperspherical front, specifically, an outgoing wave on r_3 with wave number $\kappa\sin(\alpha)$. It is then in the r_2 part that there is an approximation: the component of $\boldsymbol{\kappa}$ across the boundary is $\kappa\cos(\alpha)$ while the set $S_{n_2l_2}(r_2)$ approximates it by κ. The degree of approximation equates to that of using $\cos(\alpha) \approx 1$, carrying an error term of the order $\alpha^2/2$. This is the reason why the

particular choice $E_s = E_a$ manages, by imposing asymptotic conditions in coordinates (r_2, r_3), to approximate very well the expected hyperspherical structure. Analogously, by symmetry, the same logic applies when crossing from I to III.

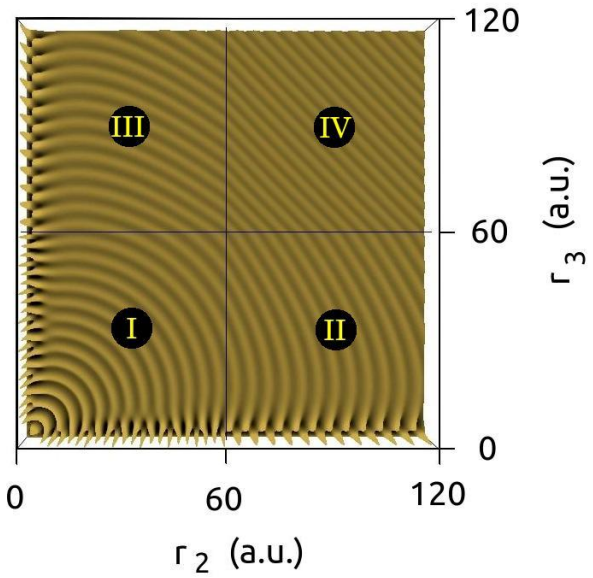

Figure 1. (Color online) Scattering wave function (real part) plotted as a function of r_2 and r_3. The calculation was performed inside a 60x60 a.u. box, but plotted in a 120x120 a.u. box. In sector II (III) the basis becomes LD in coordinate r_2 (r_3), but not in r_3 (r_2). In sector IV, the basis is LD in both coordinates.

These arguments justify the empirical affirmation made in Ref. [3], where it is suggested that taking $E_s = E_a$ provides the most precise three–body wave functions within the GSF method. We found that this choice is enough to ensure sound results to extract the transition amplitude from a region limited by $r_2, r_3 \approx 0.9\ R$, where the wave function is considerably neat and devoid of noise.

Regarding the hyperspherical double continuum, it is worth noting that hyperspherical GSF are being developed [18, 19]. In fact, coincident results for the double ionization of Helium by fast electrons with the spherical and hyperspherical GSF were jointly presented in [9]. It was suggested in [10, 20] that both versions should be mutually complementary in the sense that the single continuum information contained in the three–body wave function is better characterized with a spherical basis set, while the hyperspherical version is expected to be more efficient handling the double continuum. The hyperspherical GSF implementation is currently being generalized to go beyond the S-wave frame.

Having explained how the basis works to approximate the hyperspherical outgoing boundary conditions, we show the GSF method's consistency through a challenging test. It is very demanding for any method to solve Eq. (1) in the zero energy case ($E_a = 0$), which classically implies that both Helium electrons barely have the energy to be detached from the core. They distance themselves from the nucleus with a vanishing asymptotic velocity. This is reflected in the quantum mechanical asymptotic function described by Klar [21], with a wavelength growing with ρ:

$$\Phi^{+}_{sc}\left(\mathbf{q}, \mathbf{r}_2, \mathbf{r}_3\right) \rightarrow \frac{1}{\rho^{\frac{9}{4}}} Exp\left[A\left(\alpha, \theta\right)\sqrt{\rho}\right], \tag{6}$$

where $A(\alpha, \theta)$ depends on both, the hyperangle α and $\theta = \cos^{-1}(\widehat{\mathbf{r}}_2 \cdot \widehat{\mathbf{r}}_3)$, but not on ρ. Thus, the asymptotic hyper-momentum can be thought to be proportional to $1/\sqrt{\rho}$. Solving such a problem requires large spatial domains because the solution itself presents oscillations with very long wavelengths. For the GSF, the challenge lies in the fact that there is not a clearly convenient choice for the basis set energy E_s, since the wave vector varies with the hyperradius ρ. For the present example, the goal was to obtain a solution in a box of 170x170 a.u. using 200x200 Sturmians. We first solved the problem in a preliminary way in a 80x80 a.u. box, with a much smaller basis set (80x80 Sturmians). Then, from the last complete wave inside the preliminary domain, we took the wavelength, and from it, obtained a hyper-momentum at that radius. We finally extrapolated the hyper-momentum from ≈ 70 a.u. to ≈ 170 a.u. following the $\propto \frac{1}{\sqrt{\rho}}$ law, inferring that an energy $E_s = 0.04$ a.u. would be best suited for the bigger calculation.

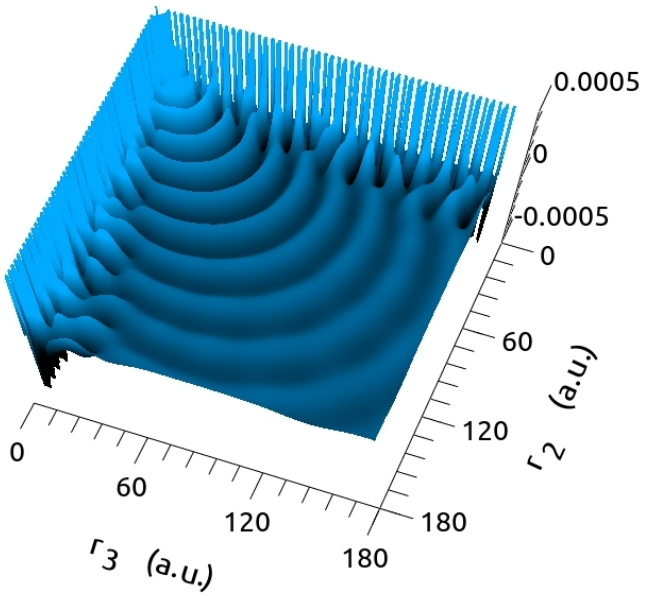

Figure 2. (Color online) Real part of the scattering wave function with zero total energy E_a and momentum transfer $q = 0.24$ a.u.

The real part of the resulting wave function is plotted in figure 2. One can appreciate how the wavelength becomes longer as the hyperradius grows, as indicated by Eq. (6). The slender structures near the two borders correspond to single ionization channels (as was studied in detail in Ref. [10]) and have been truncated in the figure to better visualize the double continuum with zero energy. Double ionization measurements are performed with two electrons emitted with a given energy which can be small (see, e.g., [22, 23]) but finite. Thus, the extreme, more challenging, case $E_a = 0$ serves here only to ensure the GSF method can handle also the very low energy regime for emitted particles.

We have in this section explained how the spherical GSF deals with the double continuum, and illustrated how it could effectively apply to very low emission energies. In the next section we will see the methodology applied to a full three–body case, namely, Eq. (1) beyond the TP approximation.

4. Application to a full three–body continuum problem

Previous work has been done by our group with respect to the long standing open problem (see, e.g., [24]) of the double ionization of Helium by high energy electrons. We first established the theoretical foundations on which we based our scattering solution [9], applied it within a TP framework, and studied the information contained in the wave function [10]. Turning to the full problem, i.e., beyond TP, we first showed results for Single Differential Cross Sections (SDCS) [11] and then for FDCS [25] in the kinematics considered experimentally by Lahmam–Bennani *et al* [12, 13, 14].

Under fast projectile and small momentum transfer kinematics, the transition matrix of the double ionization resembles that of the Double Photo Ionization (DPI) process [13, 14]. Thus, the contribution from the total angular momentum $L = 1$ wave is expected to be the dominant one. Consequently, we describe here a convergence test performed with respect to the $\{l_2, l_3\}$ partial waves corresponding to $L = 1$. The analysis was done in two runs. In the first one, we included partial waves $\{\{0,1\},\{1,2\}\{2,3\},\{3,4\}\}$, and the permuted ones $\{l_2 \leftrightarrow l_3\}$. In the second run, we used $\{\{0,1\},\{1,2\}\{2,3\},\{3,4\},\{4,5\}\}$, and their permutation. In figure 3 we show some of the partial waves contributions to $\Phi^+_{sc}(\mathbf{q}, \mathbf{r}_2, \mathbf{r}_3)$, but not the dominant ones for scale purposes. One can see that adding the $\{4,5\}$ pair produced only a very modest modification to the $\{2,3\}$ and $\{3,4\}$ waves calculated in the first run. Moreover, the amplitude of the added $\{4,5\}$ wave is significantly smaller than that corresponding to the pairs $\{0,1\}$ and $\{1,2\}$. Such a contribution would not alter the FDCS in an appreciable fashion, since the amplitudes appear squared, and waves $\{\{2,3\},\{3,4\}\}$ are already a factor ≈ 2 smaller than the dominant ones, $\{\{0,1\},\{1,2\}\}$.

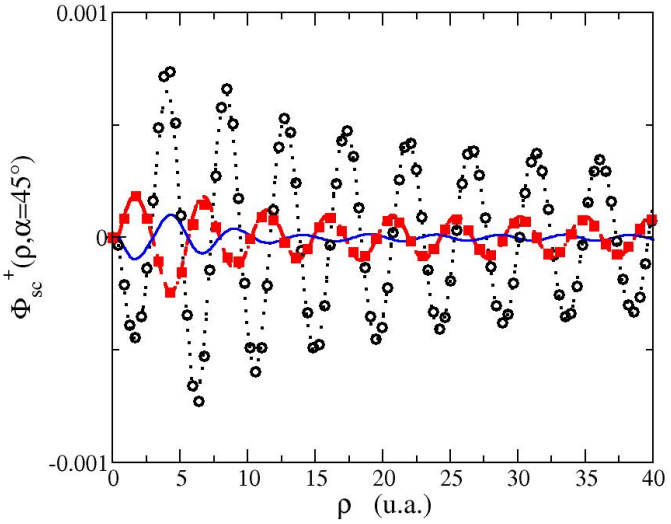

Figure 3. (Color online) Fixed hyperangle $\alpha = \pi/4$ wave function cuts (real part) for $L = 1$; the two ejected electrons possess 10 eV each, and $q = 0.24$ a.u. The wave $\{4,5\}$ (solid line) has a small magnitude when compared to waves $\{2,3\}$ (first run: open circles, second run: dotted line) and $\{3,4\}$ (first run: full squares, second run: dashed line). These waves have in turn roughly half of the amplitude of the more important $\{0,1\}$ and $\{1,2\}$ ones (not shown in the graph).

As introduced in Ref [9], the FDCS can be extracted directly from the asymptotic range of

the wave function:

$$\frac{d^5\sigma}{d\Omega_2 d\Omega_3 d\Omega_f dE_2 dE_3} = (2\pi)^3 \frac{k_f k_2 k_3}{k_i \kappa^3} \lim_{\rho\to\infty} \rho^5 |\Phi^+_{sc}(\mathbf{q}, \mathbf{r}_2, \mathbf{r}_3)|^2. \quad (7)$$

From the GSF three-body scattering wave function $\Phi^+_{sc}(\mathbf{q}, \mathbf{r}_2, \mathbf{r}_3)$ we calculated FDCS and present a contour plot in figure 4, for the coplanar Orsay kinematics [14], i.e., $E_2 = E_3 = 10$ eV ejection energies, $E_i = k_i^2/2 = 5599$ eV and $q = 0.24$ a.u.

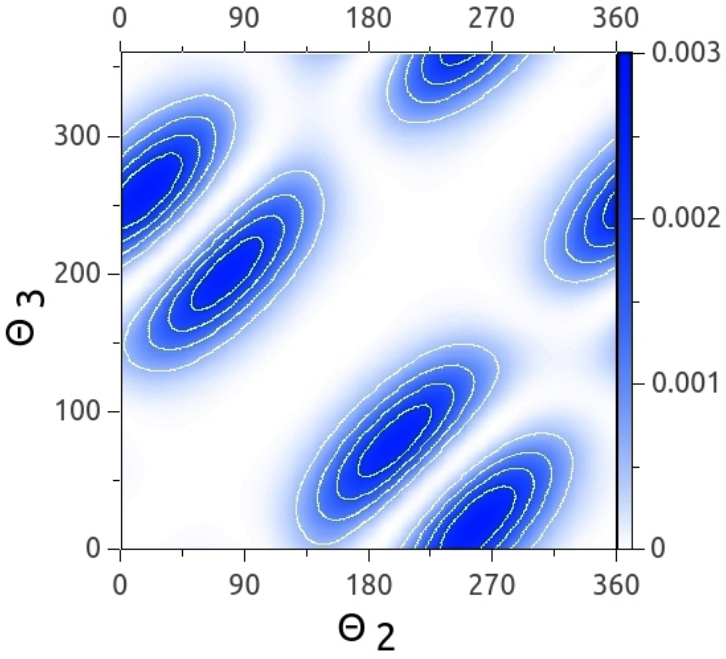

Figure 4. (Color online) Contour plot for the calculated FDCS as a function of both ejection angles θ_2 and θ_3. The kinematics are those used in the Orsay experiment [14] for (10+10) eV emission energies.

We can observe clearly the binary and recoil structures. Because of the small momentum transfer regime, those structures are expected to be present, surrounded by distinct nodal lines detailed in Ref [13]. However, the nonzero momentum transfer q implies that those peaks should not be identical. This is opposed to the DPI case where the momentum transferred to the system by the incident radiation is negligible. figure 4 shows a recoil peak that is indeed more elongated than the binary one. A deeper analysis and comparison with other theories is beyond the scope of this contribution, and can be found elsewhere [25].

5. Concluding remarks

In this contribution we detailed how the spherical GSF basis manages to deal with the three–body continuum by approximating the hyperspherical asymptotic conditions. We have justified and explained how the approach can give accurate results for three–body double continuum physical problems.

We tested the GSF basis with a zero energy problem in a Temkin–Poet model of the electron impact double ionization of Helium. This was done in order to experiment with a demanding

problem which is the extreme case of near threshold ionization. The investigation suggests that the GSF method should be able to cope also with low energy, near threshold, kinematics.

In the last section we applied the GSF to the full three–body problem, still in the fast electron impact double ionization of Helium context. The kinematics considered were those of the Orsay experiment [14]. Under the small momentum transfer regime, the double ionization transition matrix has a structure similar to that found in the dipolar DPI case. The $L = 1$ wave is the most dominant one, and as such, we presented a convergence analysis with respect to its $\{l_2, l_3\}$ waves. The FDCS calculated with the GSF method present the expected peak and nodal structure studied by Lahmam–Benanni *et al* [13]. The full analysis of the results in comparison with the experiments and other theoretical calculations are to be presented elsewhere.

Acknowledgments

We acknowledge the CNRS (PICS project No. 06304) and CONICET (project No. Dl 158114) for funding our French-Argentinian collaboration. The support by ANPCyT (PICT08/0934) (Argentina) and PIP 200901/552 CONICET (Argentina) is acknowledged. GG also thanks the support by PGI (24/F059) of the Universidad Nacional del Sur.

References

[1] Frapiccini A L, Gonzalez V Y, Randazzo J M, Colavecchia F D and Gasaneo G 2007 *Int. J. Quantum Chem.* **107** 832–844
[2] Gasaneo G, Ancarani L U, Mitnik D M, Randazzo J M, Frapiccini A L and Colavecchia F D 2013 *Adv. Quantum Chem.* **67** 153–216
[3] Randazzo J M, Buezas F, Frapiccini A L, Colavecchia F D and Gasaneo G 2011 *Phys. Rev. A* **84** 052715
[4] Randazzo J M, Frapiccini A L, Colavecchia F D and Gasaneo G 2009 *Phys. Rev. A* **79** 022507
[5] Randazzo J M, Frapiccini A L, Colavecchia F D and Gasaneo G 2009 *Int. J. Quantum Chem.* **109** 125–134
[6] Frapiccini A L, Randazzo J M, Gasaneo G and Colavecchia F D 2010 *Phys. Rev. A* **82**(4) 042503
[7] Randazzo J M, Ancarani L U, Gasaneo G, Frapiccini A L and Colavecchia F D 2010 *Phys. Rev. A* **81** 042520
[8] Frapiccini A L, Randazzo J M, Gasaneo G and Colavecchia F D 2010 *J. Phys. B* **43** 101001
[9] Gasaneo G, Mitnik D M, Randazzo J M, Ancarani L U and Colavecchia F D 2013 *Phys. Rev. A* **87** 042707
[10] Ambrosio M J, Gasaneo G and Colavecchia F D 2014 *Phys. Rev. A* **89** 012713
[11] Ambrosio M J, Ancarani L, Mitnik D, Colavecchia F and Gasaneo G 2014 *Few-Body Syst.* **55** 825–829
[12] Taouil I, Lahmam-Bennani A, Duguet A and Avaldi L 1998 *Phys. Rev. Lett.* **81** 4600–4603
[13] Lahmam-Bennani A, Taouil I, Duguet A, Lecas M, Avaldi L and Berakdar J 1999 *Phys. Rev. A* **59** 3548–3555
[14] Kheifets A, Bray I, Lahmamm-Bennani, Duguet A and Taouil I 1999 *J. Phys. B.* **32** 5047
[15] Peterkop R K 1977 *Theory of ionization of atoms by electron impact* (Colorado Associated University Press)
[16] Kadyrov A S, Mukhamedzhanov A M, Stelbovics A T, Bray I and Pirlepesov F 2003 *Phys. Rev. A* **68** 022703
[17] Kadyrov A S, Mukhamedzhanov A M, Stelbovics A T and Bray I 2004 *Phys. Rev. A* **70** 062703
[18] Gasaneo G and Ancarani L U 2012 *J. Phys. A* **45** 045304
[19] Mitnik D M, Gasaneo G and Ancarani L U 2013 *J. Phys. B* **46** 015202
[20] Mitnik D M, Gasaneo G, Ancarani L U and Ambrosio M J 2014 *J. Phys. : Conf. Ser.* **488** 012049
[21] Klar H and Schlecht W 1976 *J. Phys. B* **9** 1699
[22] Dürr M, Dorn A, Ullrich J, Cao S P, Czasch A, Kheifets A S, Götz J R and Briggs J S 2007 *Phys. Rev. Lett.* **98**(19) 193201
[23] Ren X, Dorn A and Ullrich J 2008 *Phys. Rev. Lett.* **101** 093201
[24] Ancarani L U, Cappello C D and Gasaneo G 2010 *J. Phys: Conf. Ser.* **212** 012025
[25] Ambrosio M J, Colavecchia F D, Gasaneo G, Ancarani L U and Mitnik D M 2014, submitted to *J. Phys. B*